

Commensurate Growth of Magnetite

Microinclusions in Olivine under Mantle Conditions

Marcello Campione,^{,†} Mattia La Fortezza,[†] Matteo Alvaro,[‡] Marco Scambelluri,[§] and Nadia Malaspina^{*,†}*

[†]Department of Earth and Environmental Sciences, University of Milano – Bicocca, Piazza della Scienza 4, I-20126 Milano, Italy

[‡]Department of Earth and Environmental Sciences, University of Pavia, Via A. Ferrata 1, I-27100 Pavia, Italy

[§]Department of Earth Science, Environment, and Life, University of Genova, Corso Europa 26, I-16132 Genova, Italy

KEYWORDS: serpentization, dehydration reaction, nucleation and growth, epitaxy, x-ray diffraction, reciprocal crystallographic orientations

ABSTRACT

Magnetite-bearing multiphase solid inclusions hosted in metamorphic olivine have been interpreted as final products of the trapping of the aqueous fluid produced by the subduction-zone dehydration of former serpentinites. We provide here a careful analysis performed by micro-focus single-crystal x-ray diffraction of inclusions found in harzburgites from the Almirez Complex (Béitic Cordillera, Spain) to determine the occurrence of preferential crystallographic orientation relationships between the olivine host and the magnetite inclusion. The results demonstrate that the magnetite-olivine interface selectively displays parallelism between crystallographic planes (111) and (100), and between crystallographic directions $\langle 110 \rangle$ and $\langle 011 \rangle$, respectively. This evidence points to a clear epitaxial growth of magnetite on olivine. The calculation of the geometrical misfit between the two lattices in contact as a function of their relative azimuthal orientation shows that under the aforementioned reciprocal orientation a perfect commensurism is achieved, i.e. all the nodes of the magnetite lattice coincide with nodes of the olivine lattice. This particular relationship must be interpreted as a unique occurrence, playing a fundamental role in favoring the heterogeneous nucleation of magnetite on olivine.

INTRODUCTION

Fluid inclusions trapped in minerals equilibrated or re-crystallized at high pressures in the deep Earth (pressure $p > 1$ GPa) are remnants of the fluid phases released during dehydration reactions of minerals, or by fluid-rock interaction. This type of inclusions is commonly hosted by minerals that are themselves the product of the fluid-related geologic process, such as, for instance, olivine forming by serpentine dehydration in subducted serpentinites. During subduction, the water stored in serpentinites is progressively released at increasing temperatures by the following sequence of dehydration reactions:

(1) chrysotile \pm lizardite + SiO_{2(aq)} = antigorite + fluid, occurring during early subduction ($p < 1$ GPa; temperature $T = 200\text{--}300$ °C) beneath accretionary wedges, up to 30 km depth;

(2) antigorite + brucite = olivine + fluid, occurring at eclogite facies conditions ($p = 1\text{--}2$ GPa; $T = 300\text{--}500$ °C) during the prograde subduction metamorphism up to 60 km depth. Evidence of this reaction has been described in Alpine serpentinites from Erro Tobbio (Liguria, Italy), which show rock- and vein-forming antigorite + olivine paragenesis and the occurrence of Cl, B and Li-bearing fluid inclusions in olivine and diopside;^{1,2}

(3) antigorite = olivine + orthopyroxene + chlorite + fluid, occurring at $p > 2$ GPa and $T > 550$ °C, corresponding to subduction depths exceeding 60 km in the mantle. It represents the most important dehydration reaction, releasing 5–10 wt% of H₂O in the overlying mantle wedge.³

Here we investigate natural multiphase inclusions produced by the antigorite breakdown reaction (3) hosted in chlorite harzburgites from Cerro del Almiraz (Spain) and related to the subduction-zone dehydration of serpentinite protoliths that formed the fossil Jurassic oceanic lithosphere involved in the Alpine orogeny.⁴ In these rocks, olivine produced by reaction (3) hosts several multiphase inclusions characterized by enrichments in B, Li, alkalis, Pb and Sr.⁵

The so-called multiphase inclusions generally correspond to regular microcavities in metamorphic minerals which contain a mix of microcrystalline minerals (daughter phases) wet by a fluid phase: they are traditionally interpreted either as the result of direct precipitation of the solute dissolved in the fluid, or as the result of a more complex interaction between the fluid and the host mineral (dissolution-precipitation process). As reference example, the garnet–orthopyroxenite from the Maowu Ultramafic Complex (China) formed at ~ 4 GPa and 750 °C as the result of metasomatism of former mantle harzburgite driven by a SiO₂- and H₂O-rich fluid phase. These rocks contain multiphase inclusions of the fluid evolved by fluid-rock interaction process: Campione et al.⁶

showed that the mineral assemblages inside the inclusions can be modelled in terms of thermodynamic equilibrium achieved among precipitated bulk solid phases immersed in liquid by taking into account special volume and mass constraints imposed by the host-inclusion system. Malaspina et al.^{7,8} demonstrated for the first time the presence of an epitaxial registry between the precipitated spinel mineral infilling in a garnet host. Epitaxial registry requires that interface processes, such as heterogeneous nucleation, might have an important influence on the dynamics of phase nucleation and on the mechanism that allows attaining thermodynamic equilibrium. To substantiate this hypothesis, here we show that the inclusions in metamorphic olivine formed by serpentinite dehydration at Cerro del Almirez reveal a unique case of commensurate epitaxial growth at mantle conditions of the daughter phases in magnetite-bearing multiphase solid inclusions in olivine.

METHODOLOGY

Single-crystal diffractometry has been performed at the Department of Earth and Environmental Sciences of the University of Pavia using a Rigaku Oxford Diffraction SuperNova diffractometer equipped with a Mo micro-source X-ray tube and a Dectris Pilatus-R200K detector, controlled by the CrysAlis-Pro™ software (Rigaku Oxford Diffraction). Centring of the inclusion and data collection have been performed by scanning ϕ (60°) with a scan width of 0.5° ,^{7,9} producing 120 frames with an exposure of 15 seconds. Measurements have been performed on pristine inclusions larger than $15 \mu\text{m}$ for which the signal to noise ratio allowed reliable measurements of the angular position of diffraction peaks and thus consistent determination of the orientation matrices (see Table S1). The orientation matrices have as components the reciprocal lattice vectors of the crystal with respect to the ϕ axis coordinate system of the diffractometer.¹⁰ The orientation matrices of each host and inclusions come from one measurement, therefore the orientation matrices for any

host crystal and all of its guest crystals are of the same type. With the software OrientXplot¹¹ one can process the two orientation matrices for each host inclusion pairs and determine their relative crystallographic orientation (CORs). Furthermore, OrientXplot software has been used to remove the ambiguities in the indexing of the diffraction data by applying the known symmetry of both the inclusion and host crystals.^{11,12} Stereographic projections then allow to visualize and compare the reciprocal CORs among several inclusions contained in several hosts.

As already pointed out for mg-chromite inclusions in diamond host, the full analyses of the CORs produced variations in the measured orientation of the major crystallographic axes of the inclusions relative to their hosts of less than 4° (ref ¹², Table 2). This value provides an indication of the possible uncertainty on the measurements of inclusion-host relative orientations and a useful cut-off to discriminate significant misorientations.

EpiCalc software was used to model the geometric agreement between olivine and magnetite by calculating a dimensionless potential (V/V_0)¹³ defined as follows. Surface lattices are modelled as overlapping plane waves with wavelength corresponding with surface lattice parameters. V/V_0 assumes discrete values between -0.5 and 1, according to the degree of matching between substrate and overlayer for the given azimuthal angle θ , which is the angle included between the base vectors that define the meshes of the two lattices in contact. In our case, the substrate is represented by the olivine host whereas the magnetite inclusion represents the overlayer. The values -0.5, 0, 0.5 and 1 are associated with a particular type of epitaxial register: for $V/V_0 = 1$ there will be incommensurate epitaxy, for $V/V_0 = 0.5$ point-on-line (POL) coincidence, for $V/V_0 = 0$ commensurate epitaxy (point-on-point, POP) and finally for $V/V_0 = -0.5$ there will be commensurate POL epitaxy in the case of a hexagonal substrate.¹⁴ EpiCalc also generates the

transformation matrix, which consists of a 2×2 square matrix that if multiplied to the vectors of the substrate lattice generates the vectors of the overlayer.

RESULTS AND DISCUSSION

The main microstructural feature of the studied Almirez samples is the presence of coarse, centimeter-sized, metamorphic olivine with arborescent and “spinifex – like” texture grown in the presence of abundant aqueous fluid released by the antigorite dehydration reaction (3) (see Supporting Figure S1). A first generation of olivine forms irregularly shaped clear cores, extensively overgrown by rims of a second generation of olivine with brown pleochroism, due to the presence of numerous oriented nano-inclusions of magnetite, chromite and ilmenite grown during the crystallization of olivine. The multiphase inclusions are found within both generations of olivine and show regular negative crystal shape (Figure 1). They display several tiny solid, birefringent microcrystals, along with a fluid phase and a cubic-shaped, opaque phase constituted by magnetite, which is always observed to grow in contact with the cavity walls of the olivine host mineral. Previous works¹⁵ identified the coexistence of chlorite and liquid water by Raman and scanning electron microscope analyses. Constant volume proportions are observed¹⁵ among the various tiny solid inclusions inside the cavity (30% oxides as magnetite, 50% silicate, 20% liquid).

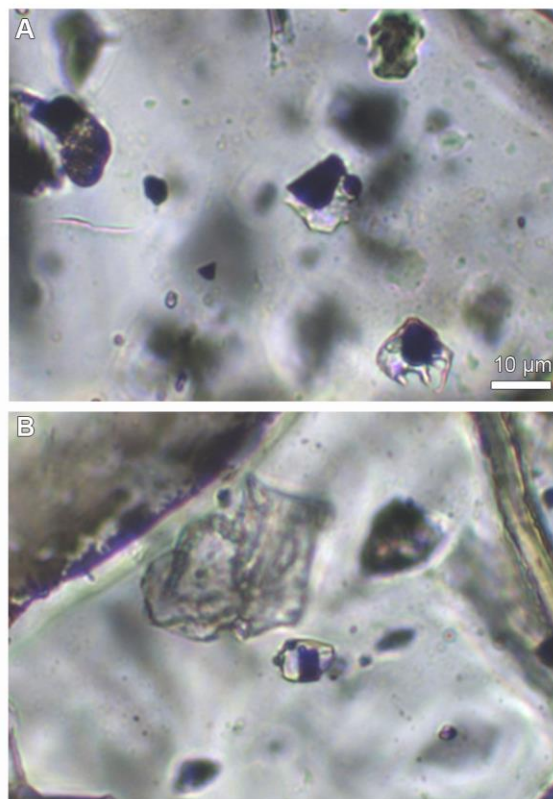


Figure 1. Optical micrographs of solid microinclusions in olivine. Magnetite microcrystals appear as an opaque phase with cubic habit growing in contact with the olivine host mineral forming a cavity with negative crystal shape. Constant volume ratios are observed between the various tiny solid inclusions and the residual fluid phase.

Micro-focused XRD was performed with the aim to characterize the crystal phases inside the inclusions by collecting diffraction patterns pertaining to a diffraction volume including all the cavity volume and a fraction of the host nearby the cavity. The crystallographic data processing was performed by indexing the diffraction peaks to obtain the UB matrix (see ref ¹⁰ for further details). The UB matrices also enable to obtain the cell parameters of the phases (see Supporting Table S1) that allow identifying them as olivine and magnetite. By combining the information of the matrices of two phases, it was possible to establish their reciprocal crystallographic orientation (CORs) with the help of the program OrientXplot.¹¹ Figure 2 reports the outcome of this analysis with the help of stereographic projections.

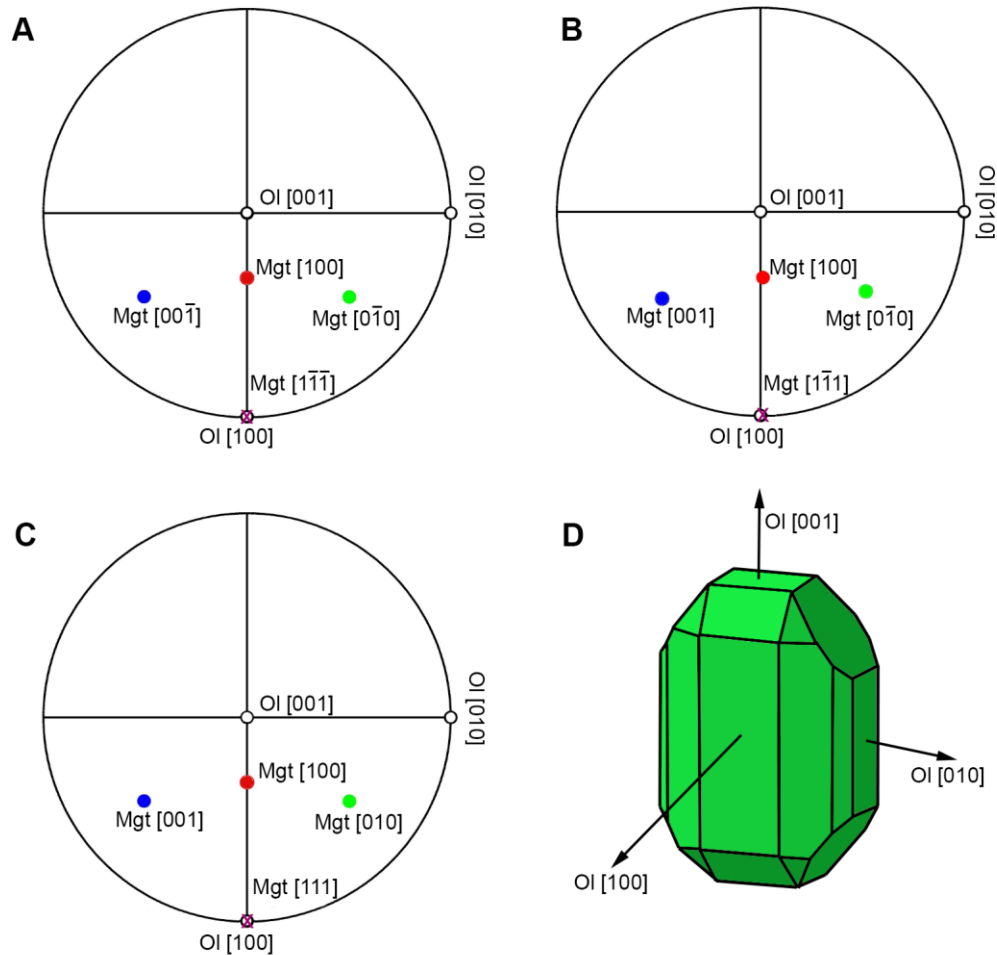


Figure 2. Stereographic projections (A-C) showing the orientation of magnetite inclusions relative to olivine host. The olivine (Ol) host is plotted with (100), (010), and (001) planes (black open dots) oriented parallel to X-, Y-, and Z-axis, respectively (D). The magnetite (mgt) (111) plane (purple cross) is systematically observed to be parallel to Ol(100) with three symmetrically equivalent relative azimuthal orientations. This indicates that the mgt(111) and Ol(100) are contact planes with a precise epitaxial registry. Blue and green dots indicate mgt(001) and mgt(010) planes.

We identified the occurrence of three symmetrically equivalent reciprocal orientations of magnetite and olivine. In these orientations, the magnetite(111) plane is always parallel to

olivine(100). This indicates that the magnetite microcrystals grew with their (111) plane in contact with olivine(100). Given these contact planes, three different yet symmetrically equivalent azimuthal orientations of the two crystals are found. Indeed, primitive crystallographic directions of magnetite are observed to be parallel to three fixed directions.

In order to understand the selection of this orientation between magnetite and olivine, we assume this be the result of an energetically favorable configuration arising from a possible lattice match between magnetite(111) and olivine(100). To analyze this match, we quantified the geometrical registry between the two lattices as a function of the azimuthal angle θ between the short surface axis of olivine and the surface axis of magnetite. This quantification was based on the algorithm used by the program EpiCalc. The results of this modelling performed for magnetite and olivine are displayed in Figure 3.

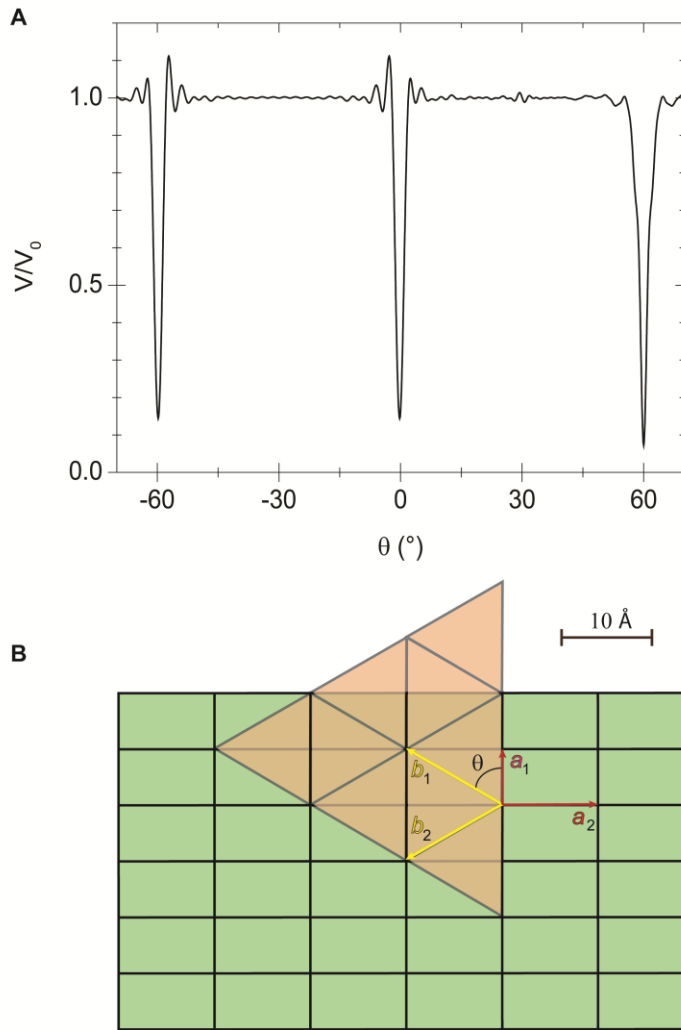


Figure 3. Geometric modelling of the agreement between magnetite and olivine deduced by calculating the lattice mismatch between magnetite(111) [brownish lattice with $b_1 = b_2 = 11.84 \text{ \AA}$] and olivine(100) [greenish lattice with $a_1 = 5.98 \text{ \AA}$ and $a_2 = 10.23 \text{ \AA}$] as a function of the azimuthal orientation θ [angle between a_1 and b_1]. Calculation was performed with the program EpiCalc which computes values of a dimensionless potential V/V_0 showing minima at angles θ ensuring a certain degree of coincidence among lattice points. At $\theta = 0$ and $\pm 60^\circ$ the dimensionless potential is observed to decrease from 1.0 down to 0.0 (panel A). This is the lowest possible value admitted and indicates commensurism of the two lattices. Indeed, e.g. for $\theta = +60^\circ$ (panel B), the matrix allowing for the conversion of the olivine lattice base vectors into those of the magnetite lattice (transformation matrix) has all integer elements $\begin{pmatrix} \mathbf{b}_1 \\ \mathbf{b}_2 \end{pmatrix} = \begin{bmatrix} 1.00 & -1.00 \\ -1.00 & -1.00 \end{bmatrix} \begin{pmatrix} \mathbf{a}_1 \\ \mathbf{a}_2 \end{pmatrix}$, indicating that all lattice points of magnetite lie on lattice points of olivine.

Clear minima of the dimensionless potential appear at $\theta = 0^\circ$ and $\pm 60^\circ$ (Figure 3A). Under these configurations, the triangular lattice of magnetite(111) is oriented in such a way that all its lattice nodes are coincident with lattice nodes of olivine (Figure 3B). The transformation matrix converting olivine lattice base vectors into those of magnetite is characterized by all integer elements. This occurrence demonstrates achievement of perfect commensurate contacts between magnetite(111) and olivine(100). Considering the different symmetry and lattice metrics of the two crystals, this commensurate relationship appears as an exceptional occurrence. Lattice coincidences among mineral phases in inclusions were already found for the spinel/pyrope system.⁷ However, such coincidences were of the POL type since only half of the lattice points of the overlaying spinel coincide with lattice points of the pyrope substrate. A POP coincidence (i.e. commensurism) as that observed in this study is the strongest and the rarest form of lattice match. Lattice match is commonly associated to an energetic advantage, in the sense that when geometric coincidence is provided between two crystal surfaces in contact this ensures maximization of attractive interactions and then minimization of interface energy.

It is reasonable to suggest that the favorable interaction between olivine(100) and magnetite(111) reduces to a great extent the energy barrier for the heterogeneous nucleation of magnetite. This reduction is the primary cause for the kinetic selection of magnetite without which, under the same conditions, magnetite nucleation would probably have been suppressed. Due to the exceptional occurrence of commensurism, this interaction might be so strong that magnetite nucleation can occur under very low level of supersaturation or even at undersaturation of the fluids.¹⁶ Commensurism is not the only way mineral infillings have been observed to organize at the host-cavity interface. For the case of garnet–orthopyroxenite from the Maowu Ultramafic Complex cited above (ref ^{7,8}), a POL registry has been observed between spinel(100) and pyrope(100).

There, the two crystals present the same cubic symmetry with the square lattices in contact having different metrics. However, the lattice parameter of spinel(100) is a factor equal to $\sin(\pi/4)$ of that of pyrope, allowing for a coincident azimuthal orientation of the two lattices. Even though this coincidence plays a similar role in promoting the nucleation of spinel, it is not so robust as the commensurism observed in the magnetite-olivine system. These considerations demonstrate that when studying multiphase inclusion systems with the purpose of deducing features of large-scale processes, it must be taken into account that interfaces might play a significant role in the formation process of mineral phases. This example of commensurate growth of magnetite on olivine demonstrates that interface energetics, together with volume properties of the minerals, control the physical appearance of reaction products. This represents a general conclusion and does not hold only within the unique environment of inclusion systems.

The studied inclusions are microsystems showing the chemical behavior of a subduction fluid during interaction with olivine in a closed system. Our study shows that the process of evolution of a fluid that is in contact with olivine is controlled by the reaction of magnetite formation, as well as the energetic cost related to the nucleation and growth of the product phases. Our results show that in spite of the crystallographic differences between magnetite and olivine, the availability of suitable lattice planes particularly facilitates the nucleation of product magnetites. This may explain the widespread occurrence of magnetite at sites of de-serpentinization.

ASSOCIATED CONTENT

Supporting Information. Optical micrographs of peridotites, XRD lattice parameters of olivine and magnetite.

The following files are available free of charge.

Figures S1, Table S1 (PDF)

AUTHOR INFORMATION

Corresponding Authors

* E.mail: marcello.campione@unimib.it, * E.mail: nadia.malaspina@unimib.it.

Author Contributions

The manuscript was written through contributions of all authors. All authors have given approval to the final version of the manuscript.

Funding Sources

University of Milano – Bicocca, FAQC grant n. 2018-ATESP-0010.

Italian Ministry of University and Research (PRIN 2017 - Prot. 2017ZE49E7_005)

ACKNOWLEDGMENT

M.C. acknowledges the financial support of the University of Milano – Bicocca with FAQC grant n. 2018-ATESP-0010. N.M, M.A. and M.S. acknowledge the financial support of the Italian Ministry of University and Research (PRIN 2017 - Prot. 2017ZE49E7_005). M.A. is thankful to Marta Morana for her help in carrying our XRD experiments.

REFERENCES

- (1) Scambelluri, M.; Piccardo, G. B.; Philippot, P.; Robbiano, A.; Negretti, L. High Salinity Fluid Inclusions Formed from Recycled Seawater in Deeply Subducted Alpine Serpentine. *Earth Planet. Sci. Lett.* **1997**, *148* (3–4), 485–499. [https://doi.org/10.1016/s0012-821x\(97\)00043-5](https://doi.org/10.1016/s0012-821x(97)00043-5).
- (2) Scambelluri, M.; Tonarini, S. Boron Isotope Evidence for Shallow Fluid Transfer across Subduction Zones by Serpentinized Mantle. *Geology* **2012**, *40* (10), 907–910. <https://doi.org/10.1130/G33233.1>.
- (3) Ulmer, P.; Trommsdorff, V. Serpentine Stability to Mantle Depths and Subduction-Related Magmatism. *Science* **1995**, *268* (5212), 858–861. <https://doi.org/10.1126/science.268.5212.858>.
- (4) Trommsdorff, V.; López Sánchez-Vizcaíno, V.; Gómez-Pugnaire, M. T.; Müntener, O. High Pressure Breakdown of Antigorite to Spinifex-Textured Olivine and Orthopyroxene, SE Spain. *Contrib. to Mineral. Petrol.* **1998**, *132* (2), 139–148. <https://doi.org/10.1007/s004100050412>.
- (5) Scambelluri, M.; Müntener, O.; Ottolini, L.; Pettke, T. T.; Vannucci, R. The Fate of B, Cl and Li in the Subducted Oceanic Mantle and in the Antigorite Breakdown Fluids. *Earth Planet. Sci. Lett.* **2004**, *222* (1), 217–234. <https://doi.org/10.1016/j.epsl.2004.02.012>.
- (6) Campione, M.; Tumiati, S.; Malaspina, N. Primary Spinel + Chlorite Inclusions in Mantle Garnet Formed at Ultrahigh-Pressure. *Geochemical Perspect. Lett.* **2017**, *4*, 19–23. <https://doi.org/10.7185/geochemlet.1730>.
- (7) Malaspina, N.; Alvaro, M.; Campione, M.; Wilhelm, H.; Nestola, F. Dynamics of Mineral

- Crystallization from Precipitated Slab-Derived Fluid Phase: First in Situ Synchrotron X-Ray Measurements. *Contrib. to Mineral. Petrol.* **2015**, *169* (3), 1–12. <https://doi.org/10.1007/s00410-015-1121-z>.
- (8) Malaspina, N.; Langenhorst, F.; Tumiati, S.; Campione, M.; Frezzotti, M. L.; Poli, S. The Redox Budget of Crust-Derived Fluid Phases at the Slab-Mantle Interface. *Geochim. Cosmochim. Acta* **2017**, *209*, 70–84. <https://doi.org/10.1016/j.gca.2017.04.004>.
- (9) Murri, M.; Cámara, F.; Adam, J.; Domeneghetti, M. C.; Alvaro, M. Intracrystalline “Geothermometry” Assessed on Clino and Orthopyroxene Bearing Synthetic Rocks. *Geochim. Cosmochim. Acta* **2018**, *227*, 133–142. <https://doi.org/10.1016/j.gca.2018.02.010>.
- (10) Busing, W. R.; Levy, H. A. Angle Calculations for 3- and 4-Circle X-Ray and Neutron Diffractometers. *Acta Crystallogr.* **1967**, *22* (4), 457–464. <https://doi.org/10.1107/s0365110x67000970>.
- (11) Angel, R.; Milani, S.; Alvaro, M.; Nestola, F. OrientXplot: A Program to Analyse and Display Relative Crystal Orientations. *J. Appl. Crystallogr.* **2015**, *48* (4), 1330–1334. <https://doi.org/10.1107/S160057671501167X>.
- (12) Nimis, P.; Angel, R. J.; Alvaro, M.; Nestola, F.; Harris, J. W.; Casati, N.; Marone, F. Crystallographic Orientations of Magnesiochromite Inclusions in Diamonds: What Do They Tell Us? *Contrib. to Mineral. Petrol.* **2019**, *174* (4), 1–13. <https://doi.org/10.1007/s00410-019-1559-5>.
- (13) Last, J. A.; Hooks, D. E.; Hillier, A. C.; Ward, M. D. The Physicochemical Origins of Coincident Epitaxy in Molecular Overlayers: Lattice Modeling vs Potential Energy Calculations. *J. Phys. Chem. B* **1999**, *103* (32), 6723–6733.

<https://doi.org/10.1021/jp984101j>.

- (14) Hooks, D. E.; Fritz, T.; Ward, M. D. Epitaxy and Molecular Organization on Solid Substrates. *Adv. Mater.* **2001**, *13* (4), 227–241. [https://doi.org/10.1002/1521-4095\(200102\)13:4<227::AID-ADMA227>3.0.CO;2-P](https://doi.org/10.1002/1521-4095(200102)13:4<227::AID-ADMA227>3.0.CO;2-P).
- (15) Scambelluri, M.; Bottazzi, P.; Trommsdorff, V.; Vannucci, R.; Hermann, J.; Gómez-Pugnaire, M. T.; López-Sánchez Vizcano, V. Incompatible Element-Rich Fluids Released by Antigorite Breakdown in Deeply Subducted Mantle. *Earth Planet. Sci. Lett.* **2001**, *192* (3), 457–470. [https://doi.org/10.1016/S0012-821X\(01\)00457-5](https://doi.org/10.1016/S0012-821X(01)00457-5).
- (16) Mutaftschiev, B. *The Atomistic Nature of Crystal Growth*; Springer Series in Materials Science; Springer Berlin Heidelberg: Berlin, Heidelberg, 2001; Vol. 43. <https://doi.org/10.1007/978-3-662-04591-6>.

Table Of Content Image

